Nonprimed and DYRK1A-primed GSK3β-phosphorylation sites on MAP1B regulate microtubule dynamics in growing axons

Timothy M. E. Scales, Shen Lin, Michaela Kraus, Robert G. Goold* and Phillip R. Gordon-Weeks‡

The MRC Centre for Developmental Neurobiology, New Hunt's House, Guy's Campus, King's College London, London SE1 1UL, UK

*Present address: Institute of Child Health, University College London, 30 Guilford Street, London WC1N 1EH, UK

‡Author for correspondence (e-mail: phillip.gordon-weeks@kcl.ac.uk)

Accepted 21 April 2009

Journal of Cell Science 122, 2424-2435 Published by The Company of Biologists 2009

doi:10.1242/jcs.040162

Summary

MAP1B is a developmentally regulated microtubule-associated phosphoprotein that regulates microtubule dynamics in growing axons and growth cones. We used mass spectrometry to map 28 phosphorylation sites on MAP1B, and selected for further study a putative primed GSK3β site and compared it with two nonprimed GSK3β sites that we had previously characterised. We raised a panel of phosphospecific antibodies to these sites on MAP1B and used it to assess the distribution of phosphorylated MAP1B in the developing nervous system. This showed that the nonprimed sites are restricted to growing axons, whereas the primed sites are also expressed in the neuronal cell body. To identify kinases phosphorylating MAP1B, we added kinase inhibitors to cultured embryonic cortical neurons and monitored MAP1B phosphorylation with our panel of phosphospecific antibodies. These experiments identified dual-specificity tyrosine-phosphorylation-regulated kinase (DYRK1A) as the kinase that primes sites of GSK3β phosphorylation in MAP1B, and we confirmed this by knocking down *DYRK1A* in cultured embryonic cortical neurons by using shRNA. *DYRK1A* knockdown compromised neuritogenesis and was associated with alterations in microtubule stability. These experiments demonstrate that MAP1B has DYRK1A-primed and nonprimed GSK3β sites that are involved in the regulation of microtubule stability in growing axons.

Key words: Neuritogenesis, MAP1B, GSK3β, DYRK1A, Microtubule dynamics, Mass spectrometry

Introduction

MAP1B is a developmentally regulated, microtubule-associated phosphoprotein that is expressed at high levels in differentiating neurons and in regions of the adult nervous system that show neuronal plasticity or regenerate after injury (reviewed by Gordon-Weeks and Fischer, 2000; Riederer, 2007). Although it is clear that MAP1B plays an important role in neurite growth, growth-cone function and neuronal migration, and is implicated in a number of neurological disorders, such as fragile X syndrome (Lu et al., 2004) and giant axonal neuropathy (Allen et al., 2005), the underlying molecular mechanisms are unknown (reviewed by Gonzalez-Billault et al., 2004; Halpain and Dehmelt, 2006). Mouse knockouts suggest that MAP1B plays a role in neuronal migration, neuritogenesis and, possibly, in growth-cone pathfinding (Gonzalez-Billault and Avila, 2000). This idea is consistent with the finding that MAP1B is downstream of various signalling pathways that stimulate neurite growth or direct growth-cone pathfinding, e.g. laminin (DiTella et al., 1996; Paglini et al., 1998), netrins (Del Rio et al., 2004), neurotrophins (Goold and Gordon-Weeks, 2001; Goold and Gordon-Weeks, 2003; Goold and Gordon-Weeks, 2005) and Wnts (Lucas et al., 1998; Ciani et al., 2004), or that influence neuronal migration, e.g. reelin (Gonzalez-Billault et al., 2005).

A number of kinases have been proposed to phosphorylate MAP1B, including casein kinase 2 (CK2) (Díaz-Nido et al., 1988; Ulloa et al., 1993), cyclin-dependent kinase 5 (Cdk5) (DiTella et al., 1996; Paglini et al., 1998; Pigino et al., 1997; Hahn et al., 2005), Jun terminal kinase (JNK) (Chang et al., 2003; Kawauchi et al., 2003; Kawauchi et al., 2005) and glycogen synthase kinase 3β (GSK3β) (Lucas et al., 1998; Goold et al., 1999; Goold and Gordon-Weeks, 2001; Trivedi et al., 2005; Kim et al., 2006). However, evidence for a direct phosphorylation only exists for GSK3β, and two phosphorylation sites in mouse MAP1B, S1260 and T1265, have been mapped (Trivedi et al., 2005). The physiological function of phosphorylation is not clear, although there is indirect evidence that it might regulate the control that MAP1B exerts on microtubule dynamics (Goold et al., 1999; Trivedi et al., 2005). There is evidence that CK2- and GSK3β-phosphorylated MAP1B can bind to microtubules (Díaz-Nido et al., 1988; Goold et al., 1999; Goold and Gordon-Weeks, 2001), whereas JNK-phosphorylated MAP1B does not bind to microtubules (Chang et al., 2003).

We used a phosphoproteomic approach to map phosphorylation sites on MAP1B and found extensive phosphorylation at serine and threonine sites, the majority of which are followed immediately downstream by a proline. We selected for further study a putative primed GSK3β-phosphorylation site and compared it with two non-primed GSK3β sites that we had previously characterised (Trivedi et al., 2005). We show that the site is indeed primed, by dual-specificity tyrosine-phosphorylation-regulated kinase (DYRK1A), and that it is involved in the regulation that MAP1B exerts on microtubule dynamics in growing axons and growth cones.

Results

A comparison of the phosphorylation maps of juvenile and adult MAP1B

We purified MAP1B from neonatal rat brain (Johnstone et al., 1997) and mapped the phosphorylation sites by mass spectrometry. This

analysis uncovered 25 phosphorylation sites and a further three sites whose precise location is ambiguous (see Table 1). The total sequence coverage of the MAP1B heavy chain was 78%, assuming the C-terminus of the heavy chain in rat MAP1B to be at amino acid 2210 (Tögel et al., 1998). We were unable to obtain sequence from the domain near the N-terminus that has an imperfect repeat motif of KKE[I/V] and resides within the microtubule-binding domain of the heavy chain (Fig. 1) (Noble et al., 1989). We compared our phosphorylation map of neonatal MAP1B with maps from embryonic (Ballif et al., 2004) and adult (Collins et al., 2005; Trinidad et al., 2005; Trinidad et al., 2006) brain. This revealed that there are both shared and unique phosphorylation sites in juvenile and adult MAP1B (Table 1). Of the 25 unambiguous sites that we found in juvenile MAP1B, nine sites were not found in adult MAP1B (Table 1). There are 19 unambiguous sites in adult MAP1B that were not found in juvenile MAP1B (Collins et al., 2005; Trinidad et al., 2005; Trinidad et al., 2006). There are five phosphorylation sites in the Ballif et al. (Ballif et al., 2004) embryonic mouse brain data set that we did not find in our neonatal rat MAP1B, despite sequencing peptides containing four of these sites (Table 1). Four of these sites are present in the data set for adult MAP1B phosphorylation (Collins et al., 2005; Trinidad et al., 2005; Trinidad et al., 2006). This suggests that there might be differences in phosphorylation sites between embryonic, neonatal and adult MAP1B, and that there might be a progressive, albeit small, increase in phosphorylation sites over developmental time. All of the confirmed sites that we found in juvenile MAP1B are either serines or threonines, and 22 out of 25 (88%) of these are followed immediately downstream by a proline. The three exceptions are: S540, which is followed by an arginine; S823, which is followed by a serine that precedes a proline and is also phosphorylated; and S1008, which is followed by glutamic acid (Table 1). One of the ambiguous sites is a tyrosine (Y934, Table 1); however, there is no biochemical evidence that MAP1B is phosphorylated on tyrosine residues (Gordon-Weeks and Fischer, 2000).

We have recently mapped two GSK3β-phosphorylation sites on juvenile mouse MAP1B to S1260 and T1265 (Trivedi et al., 2005). We confirmed the presence of phosphorylated S1260 in the mass-spectrometry data set (S1256 in the rat, Table 1) but did not find peptides containing phosphorylated T1265, probably because the proteases we used do not generate suitably sized proteolytic fragments containing this site (Table 1). Ballif et al. (Ballif et al., 2004), Collins et al. (Collins et al., 2004) and Trinidad et al. (Trinidad et al., 2005; Trinidad et al., 2006) also failed to recover peptides containing phosphorylated T1265. This finding highlights an important deficiency of mass spectrometry in identifying phosphorylation sites. We did not examine the light chain, LC1, for phosphorylation sites (Fig. 1) (Hammarback et al., 1991).

The MAP1B molecule has an extended configuration, as judged by rotary shadowing (Sato-Yoshitake et al., 1989), and so we examined the distribution of these phosphorylation sites along the MAP1B sequence to look for patterns in their distribution and relation to known motifs and binding sites (Fig. 1). This revealed a notable paucity of phosphorylation sites in the region upstream of the KKE[I/V] repeats in the microtubule-binding domain. Four phosphorylation sites were found in the flanking regions of the KKE[I/V] repeats, two on either side: T526 and S540 in the N-

Table 1. Phosphorylation sites of juvenile MAP1B

Peptide sequence	Confirmed site	Ambiguous site
ATVVVEATEPEPSGSIGNPAATTSPSLSHR	S25	
DLTGQVSTPPVK	T526	
ADSRESLKPATKPLSSK	S540†	
ELEAERSLMSSPEDLTKDFEELKAEEIDVAK	S823#, S824#	
DEEKLKETEPGEAYVIQKETEVSKGSAESP	S883	
QGVDDIEKFEDEGAGFEESSEAGDYEEKAETEEAEEPEEDGEDNVSGSASK	–	S928, S929*, Y934, T940
DEALEKGEAEQSEEEGEEEE	S1008†	
TQSTIEISSEPTPMDEMSTPRDVMTDETNNEETESPSQEFVNITKY	S1147*	
DYNASASTISPPSSMEEDKFSK	S1200	
SPSLSPSPPSPIEK	S1256#,*,†	
SVNFSLTPNEIK	T1273	
ASAEGEATAVVSPGVTQAVVEEHCASPEEK	S1304#,†	
SSISPMDEPVPDSESPIEK	–	S1367, S1368#, S1370#,*
VLSPLRSPPLIGSESAYEDFLSADDK	S1388#,*,†, S1392#,*	
QGFSDKESPVSDLTSDLYQDK	S1435†	
KLGGDGSPTQVDVSQFGSFKEDTK	S1493*,†	
DDVSPSLHAEVGSPHSTEV	S1571	
SEQSSMSIEFGQESPEHSLAMDFSR	S1644	
VQSLEGEKLSPK	S1770#,†	
ESSPTYSPGFSDSTSGAK	S1784*	
ESTAAYQTSSSPPIDAAAAEPYGFR	–	S1801, T1802#
DSTSGAKESTAAYQTSSSPPI	S1810	
TPGDFNYAYQKPESTTESPDEEDYDYESHEK	S1872#	
TTRTPEEGGYSYEISEK	T1940#,†	
SYETTTKTTRSPDTSAY	S2025#	
CYTPERKSPSEAR	S2063†	
TELSPSFINPNPLEWFAGEEPTEESERPLTQSGGAPPPSGGK	S2089#	

Phosphorylation sites in rat MAP1B identified by tandem mass spectrometry. The table shows the peptide sequences identified by tandem mass spectrometry and, in red, the phosphorylated amino acids. In peptides in which there are ambiguous sites, only one of the listed sites is phosphorylated but which one was not able to be determined. Amino acids in green were phosphorylated in the Baliff et al. (Baliff et al., 2004) data set from embryonic mouse brain.

†Also present in Trinidad et al. (Trinidad et al., 2005; Trinidad et al.2006) data set from adult mouse post-synaptic densities.

#Also present in Collins et al. (Collins et al., 2005) data set from adult mouse synaptosomes.

*Also present in Ballif et al. (Baliff et al., 2004) data set.

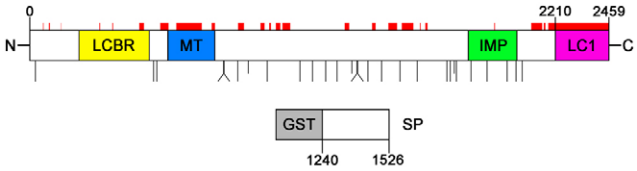

Fig. 1. Distribution of phosphorylation sites identified by tandem mass-spectrometry in juvenile-rat MAP1B. Each long vertical black line represents an unambiguously identified phosphorylation site on rat MAP1B (the three shorter black lines indicate the position of the first, N-terminal most, of each of the three ambiguous phosphorylation site groups) (see Table 1). Also shown are the positions of the microtubule-binding domain (MT), the imperfect repeats (IMP), the light chain (LC1) of MAP1B and the light-chain-binding region (LCBR) (Noiges et al., 2006). Regions of MAP1B sequence not covered by mass spectrometry are shown by red bars. Also shown is the recombinant GST-MAP1B fusion protein (SP) used in the protein-kinase assay. Although SP is derived from mouse, the numbering is for rat. The diagram is drawn to scale.

terminal flanking region, and S823 and S824 in the C-terminal flanking region (Fig. 1). In the N-terminal region of MAP1B that binds to light chain 1 (Hammarback et al., 1991; Tögel et al., 1998; Noiges et al., 2006), there are no phosphorylation sites, whereas there are two phosphorylation sites (T526 and S540) in the region in which the GABAc ρ1 neurotransmitter receptor binds (Hanley et al., 1999) (Fig. 1).

Production and characterisation of phosphospecific antibodies to MAP1B

Many GSK3β-phosphorylation sites require prior phosphorylation of a serine or threonine four (Doble and Woodgett, 2003) or five (Cole et al., 2006) amino acid residues downstream of the phospho-acceptor amino acid – the so-called priming site. These phosphorylated serines and/or threonines are usually followed immediately downstream by a proline. Inspection of the juvenile rat MAP1B-phosphorylation data set revealed the presence of a single putative primed GSK3β-phosphorylation site at S1388,S1392 (GSK3β-phosphorylation site/priming site) (Table 1). Note, however, that there is also a putative primed site at S1784,S1788, although phosphorylated S1788 has only been reported in the Baliff et al. (Baliff et al., 2004) data set (Table 1). We raised rabbit polyclonal antibodies (pAbs) to phosphorylated S1388 (S1388-*P*) and S1392-*P*, and affinity purified the antibodies. We previously raised two rabbit pAbs, BUGS and SuperBUGS, to two phosphorylation sites in mouse MAP1B, S1260 (S1256 in rat) and T1265 (T1261 in rat), respectively, that we had mapped using in vitro protein-kinase assays and site-directed mutagenesis (Trivedi et al., 2005). We used this panel of four phosphospecific, affinity-purified antibodies to further characterise the MAP1B phosphorylation sites that they recognise.

Western immunoblotting studies showed that all four antibodies recognise a single band co-migrating with MAP1B in tissue extracts from early postnatal rat brain (Fig. 2A). To determine the phospho-specificity of these antibodies, we assessed their binding to native MAP1B in the presence of phospho-peptides (Fig. 2B) and to recombinant MAP1B proteins following phosphorylation in vitro (Fig. 2C). The binding of all four antibodies to native MAP1B in extracts of neonatal rat brain was completely inhibited by prior incubation with the appropriate phosphorylated, but not with the non-phosphorylated, peptide (Fig. 2B). Furthermore, pAbs against S1388-*P* and S1392-*P* recognise a recombinant GST-MAP1B fusion protein called SP (Fig. 1) – corresponding to mouse MAP1B

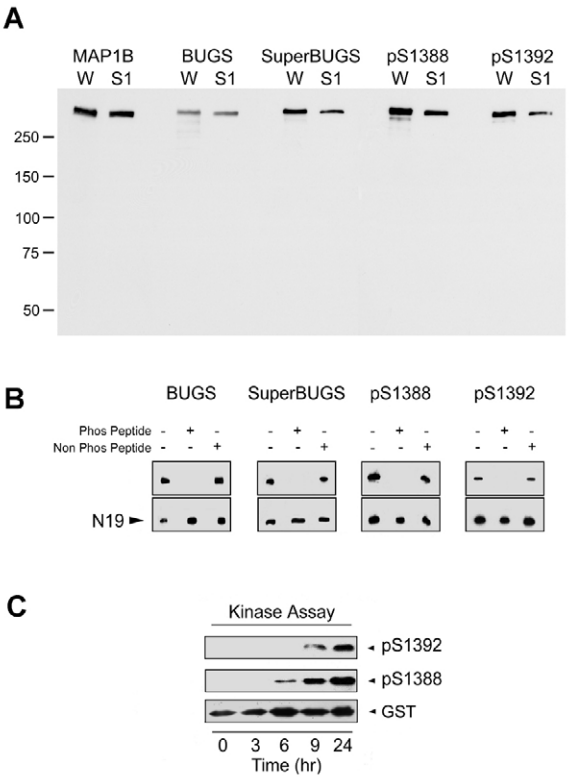

Fig. 2. Phospho-specificity of polyclonal antibodies raised to putative sites of GSK3β phosphorylation on MAP1B. (A) Affinity-purified pAbs against mouse MAP1B S1260-*P* (BUGS) and S1265-*P* (SuperBUGS), and against rat S1388-*P* and S1392-*P* were immunoblotted against proteins from neonatal rat whole brain (W) or neonatal rat brain supernatant (S1). All of these antibodies recognise a protein that co-migrates with MAP1B (~320 kDa), as indicated by comparison with protein bands recognised by pAb anti-MAP1B-C1, which recognises all forms of MAP1B (Johnstone et al., 1997). (B) Phospho-peptide inhibition assay. Pre-incubation of antibodies with the appropriate phosphorylated peptide (Phos Peptide) blocks antibody binding to native MAP1B, whereas non-phosphorylated peptide (Non Phos Peptide) has no effect. Lane 1, antibody alone; lane 2, antibody incubated with phosphorylated peptide; lane 3, antibody incubated with non-phosphorylated peptide. Peptide concentration was 8 μM, except for BUGS, for which 0.8 μM was used. N19, pAb against MAP1B. (C) A recombinant MAP1B protein (SP; Fig. 1) containing S1388 and S1392 was phosphorylated in an in vitro kinase assay and tested for immunoreactivity with pAbs against S1388-*P* and S1392-*P*. These pAbs only recognised the SP recombinant protein after it had become phosphorylated in the protein-kinase assay (6-9 hours), showing that these antibodies are phosphospecific. Blots were stripped and probed with an antibody against GST to show the level of SP (GST).

amino acids 1244-1530, and therefore containing the S1388 and S1392 sites (Trivedi et al., 2005) – only after it has been phosphorylated in vitro with a neonatal rat brain extract containing MAP1B kinases (Fig. 2C) (Johnstone et al., 1997). We have previously shown that this is also true of SuperBUGS and BUGS (Trivedi et al., 2005). We conclude, therefore, that all four antibodies are specific for phosphorylation epitopes on MAP1B.

Embryonic-spinal-cord expression of phosphorylated MAP1B

In a previous study, we showed that BUGS and SuperBUGS specifically labelled growing axons in rat embryonic spinal cord (Trivedi et al., 2005). Here, we analysed the labelling of embryonic-spinal-cord sections by pAbs S1388-*P* and S1392-*P*, and compared it with the BUGS and SuperBUGS labelling (Fig. 3) (Trivedi et al.,

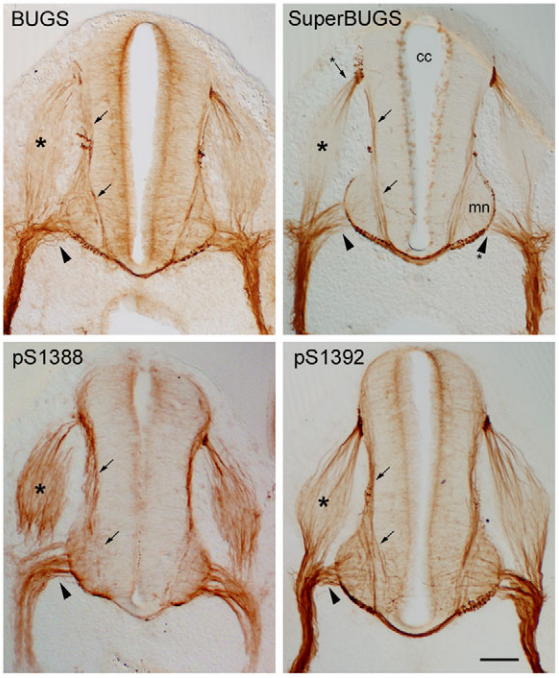

Fig. 3. MAP1B phosphorylation isoforms in embryonic rat spinal cord are restricted to growing axons. Transverse sections of embryonic rat spinal cord immunolabelled with antibodies against phosphorylation epitopes on MAP1B. All antibodies specifically label the axons of differentiating neurons in the spinal cord, including those of commissural neurons (arrows), motor neurons (arrowheads) and sensory neurons in the dorsal root ganglion (asterisks). SuperBUGS uniquely labels only the distal ends of growing axons; note the absence of labelling of the proximal regions of motor-neuron axons in the ventral horn (mn) and the proximal roots (arrowhead asterisk). Note also that only the axons at the poles of the dorsal root ganglion are labelled by SuperBUGS (arrow asterisk). By contrast, pAbs against S1388-*P* and S1392-*P* labelled axons along their entire length, and both antibodies faintly labelled neuronal cell bodies, pAb against S1388-*P* more strongly than pAb against S1392-*P*. The labelling with BUGS was intermediate between these two; neuronal cell bodies were not labelled. As noticed previously (Trivedi et al., 2005), SuperBUGS labels mitotic cells in the ventricular zone near the central canal (cc). Scale bar: 100 μm.

2005). Although all of these antibodies specifically labelled the axons of differentiating neurons in the embryonic spinal cord, there were subtle differences in the labelling pattern between antibodies. SuperBUGS labelled axons in a gradient that was highest distally. pAbs against S1388-*P* and S1392-*P* labelled axons along their entire length, whereas BUGS labelling was intermediate between these two labelling patterns, with some axons labelled in a gradient (Fig. 3). As reported previously, BUGS and SuperBUGS only labelled axons – neuronal cell bodies were unlabelled – despite the fact that MAP1B is expressed in all cellular compartments in neurons as indicated by labelling with pAb N19, which labels all forms of MAP1B (data not shown) (Trivedi et al., 2005). However, pAbs against S1388-*P* and S1392-*P* did label neuronal cell bodies, although very lightly.

GSK3β phosphorylates MAP1B at S1260 and T1265 in embryonic cortical neuronal cultures

We investigated the kinases phosphorylating MAP1B in neuronal cultures from embryonic cortex by applying kinase inhibitors to cultures and probing protein extracts from the cultures with our panel of MAP1B phosphospecific antibodies (Fig. 4). We have shown previously that GSK3β phosphorylates MAP1B at the sites recognised by BUGS and SuperBUGS (Trivedi et al., 2005). Our evidence included the observation that lithium, a non-competitive inhibitor of GSK3β (Klein and Melton, 1996; Stambolic et al., 1996), inhibited phosphorylation of the sites recognised by these antibodies in an in vitro protein-kinase assay with a recombinant MAP1B protein (Johnstone et al., 1997; Trivedi et al., 2005). We therefore predicted that GSK3β inhibitors would also inhibit phosphorylation of these sites on MAP1B in cortical cultures. We found that, indeed, lithium and TDZD-8, a highly specific non-ATP-competitive inhibitor of GSK3β (Martinez et al., 2002), reduced the binding of BUGS and SuperBUGS to MAP1B in cortical cultures (Fig. 4A), independently confirming our previous findings (Trivedi et al., 2005).

DYRK1A primes S1388, a GSK3β-phosphorylation site on MAP1B, by phosphorylating S1392 in embryonic cortical neuronal cultures

The S1388 site, identified by mass spectrometry in this study, has all the features of a classical primed GSK3β site, i.e. it is four residues upstream of S1392-*P* and both phosphorylated serines are followed immediately downstream by proline (Doble and Woodgett, 2003). We therefore predicted that GSK3β inhibitors would reduce or abolish S1388 phosphorylation but not affect S1392 phosphorylation. We found that indeed the GSK3β inhibitors lithium and TDZD-8 inhibited phosphorylation of S1388 in MAP1B in cortical cultures, but that these compounds did not inhibit S1392 phosphorylation, as determined by pAb S1392-*P* binding; in fact, they slightly increased phosphorylation at this site (Fig. 4B).

To identify the kinase phosphorylating S1392, and therefore the potential priming kinase for the GSK3β phosphorylation of S1388, we tested the effects of small-molecule inhibitors of kinases already implicated in MAP1B phosphorylation (Cdk5, CK2 and JNK). The CK2 inhibitor DMAT (Martinez et al., 2002) was without effect at either S1388 or S1392 (not shown). Surprisingly, treatment of cultured neurons with the JNK inhibitor SP600125 (Bennett et al., 2001) reduced the phosphorylation of S1388 but had no effect on S1392 phosphorylation (Fig. 4B). Furthermore, the combined use of lithium and SP600125 reduced S1388 phosphorylation to a greater extent than either lithium or SP600125 alone (Fig. 4B), suggesting that GSK3β and JNK are in separate pathways that phosphorylate S1388 in MAP1B. We found similar effects of SP600125 on the BUGS and SuperBUGS sites (Fig. 4A), indicating that the dual usage of phosphorylation sites by GSK3β and JNK might be a general phenomenon. These findings are consistent with the idea that S1388 is phosphorylated by both GSK3β and JNK, and that S1392 might be phosphorylated by another kinase.

We then tested the Cdk5 inhibitor purvalanol, a more potent inhibitor than olomoucine or roscovitine (Bain et al., 2003), in cortical cultures. Purvalanol had no effect on the BUGS and SuperBUGS sites, but it strongly reduced phosphorylation at the S1392 site and increased the phosphorylation of the S1388 site (Fig. 4A,B). This suggests that Cdk5 phosphorylates S1392 and is, therefore, potentially the priming kinase for the GSK3β-phosphorylation site at S1388. However, purvalanol also inhibits DYRK-family kinases, including DYRK1A and DYRK2 (Bain et al., 2003); these two kinases have recently been shown to prime GSK3β phosphorylation sites on tau (Woods et al., 2001) and collapse response mediator protein (CRMP) (Cole et al., 2006), respectively. We therefore compared the effects of purvalanol with the Cdk5 inhibitor roscovitine (Bain et al., 2003) and the DYRK1A

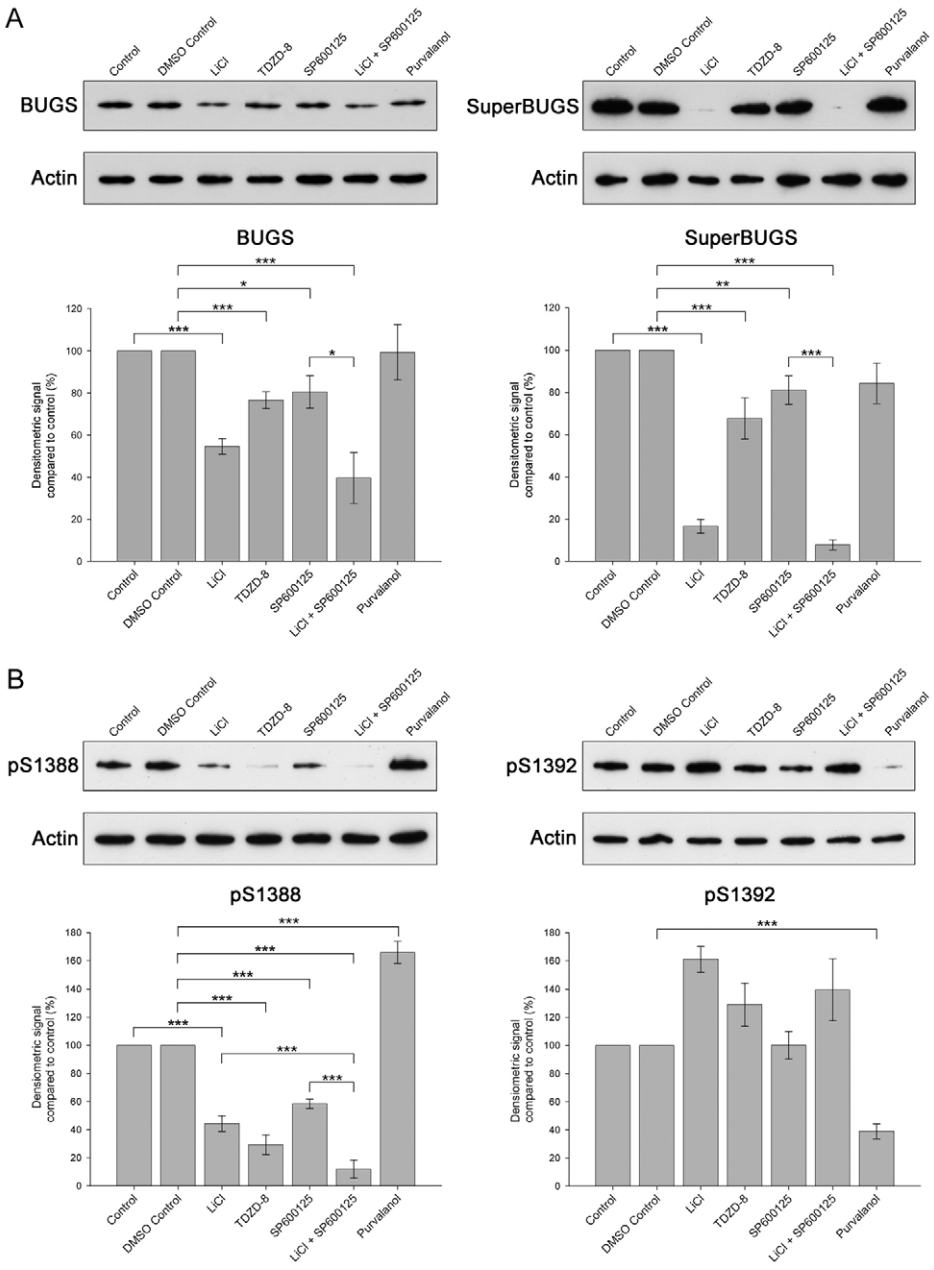

Fig. 4. Phosphorylation of S1392 on MAP1B in embryonic cortical neurons primes the phosphorylation of S1388 by GSK3β. Embryonic cerebral cortical neurons were cultured for 3 days and then treated with various kinase inhibitors for 3 hours, after which cultures were harvested for immunoblot analysis. (A) Representative immunoblots of samples from cortical cultures treated with NaCl (20 mM; Control), dimethyl sulphoxide (DMSO Control, 0.2%), LiCl (20 mM), TDZD-8 (5 μM), SP600125 (10 μM), LiCl and SP600125 (10 mM and 10 μM, respectively) or purvalanol (10 μM) and probed with the pAbs BUGS or SuperBUGS, or anti-β-actin (Actin), as a loading control. Histogram shows quantification of immunoblots from three or more independent experiments. Error bars are s.e.m. for three or more independent experiments. **P*<0.05, ***P*<0.01, ****P*<0.001. (B) Representative immunoblots of samples from cortical cultures treated with the agents as shown in A and probed with antibodies against S1388-*P*, S1392-*P* or β-actin (loading control). Histogram shows quantification of immunoblots from three or more independent experiments. Error bars are s.e.m. for three or more independent experiments. **P*<0.05, ***P*<0.01, ****P*<0.001.

inhibitor epigallocatechin-3-gallate (EGCG) (Bain et al., 2003) to try and distinguish between an involvement of Cdk5 and DYRK1A (Fig. 5). We found that EGCG, similar to purvalanol, strongly reduced phosphorylation at the S1392 site and increased the phosphorylation of the S1388 site (Fig. 5). Roscovitine, however, only slightly reduced S1392 phosphorylation and had no effect on S1388 phosphorylation. These findings strongly suggest that DYRK1A, and not Cdk5, is the priming kinase phosphorylating S1392.

Knockdown of DYRK1A in cortical neurons with shRNA confirms that DYRK1A primes GSK3β phosphorylation of MAP1B

We screened a panel of five shRNA sequences targeted against DYRK1A for an ability to knockdown DYRK1A in cultured cortical neurons following transfection. We first assessed the levels of DYRK1A using immunoblotting and selected the shRNA plasmid (*DYRK1A* shRNA) that produced the greatest reduction of DYRK1A and, as a control, an shRNA plasmid (Ctrl shRNA) that produced no reduction of DYRK1A (Fig. 6). *DYRK1A* shRNA reduced DYRK1A protein levels in cortical neurons by greater than 70% 3 days after transfection, as shown by quantitative immunoblotting (Fig. 6A). By contrast, transfection with Ctrl shRNA did not alter DYRK1A protein levels (Fig. 6A). Knockdown of DYRK1A was associated with marked reductions in the phosphorylation of S1392 (Fig. 6B) and S1388 (Fig. 6C), whereas transfection with Ctrl shRNA had no effect on the phosphorylation of these sites (Fig. 6B,C). Neither shRNAs affected the phosphorylation of the BUGS or SuperBUGS sites (not shown). These findings independently confirm that DYRK1A primes the GSK3β phosphorylation of S1388 in MAP1B by phosphorylating S1392 (Fig. 6). DYRK1A also phosphorylates the microtubule-associated protein tau, at T212

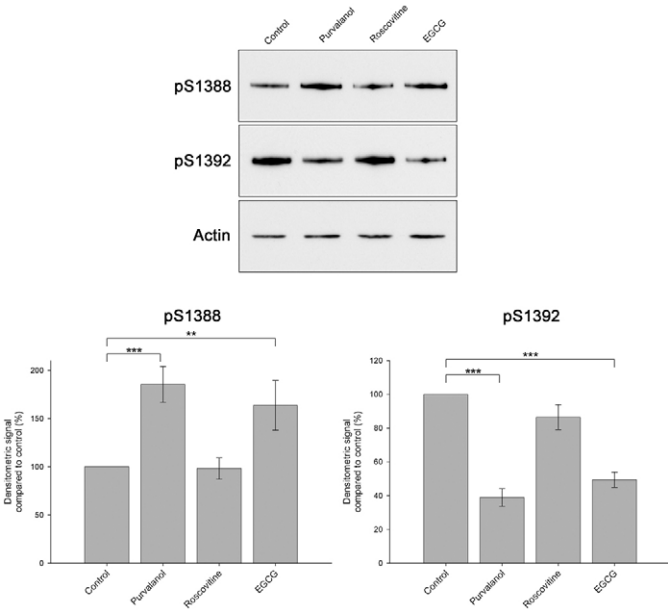

Fig. 5. Pharmacological evidence that DYRK1A phosphorylates S1392 and primes the phosphorylation of S1388 by GSK3β. Representative immunoblots of samples from cortical cultures treated with dimethyl sulphoxide (0.2%, Control), purvalanol (10 μM), roscovitine (20 μM) or EGCG (50 μM) and probed with pAbs against S1388-*P* or pS1392-*P* or anti-β-actin (Actin), as a loading control. Both purvalanol and EGCG increase S1388 phosphorylation, whereas roscovitine has no effect. Similarly, purvalanol and EGCG substantially reduce S1392 phosphorylation, whereas roscovitine has little effect. Histogram shows quantification of immunoblots from three or more independent experiments. Error bars are s.e.m. for three or more independent experiments. $^{**}P<0.01$, $^{***}P<0.001$.

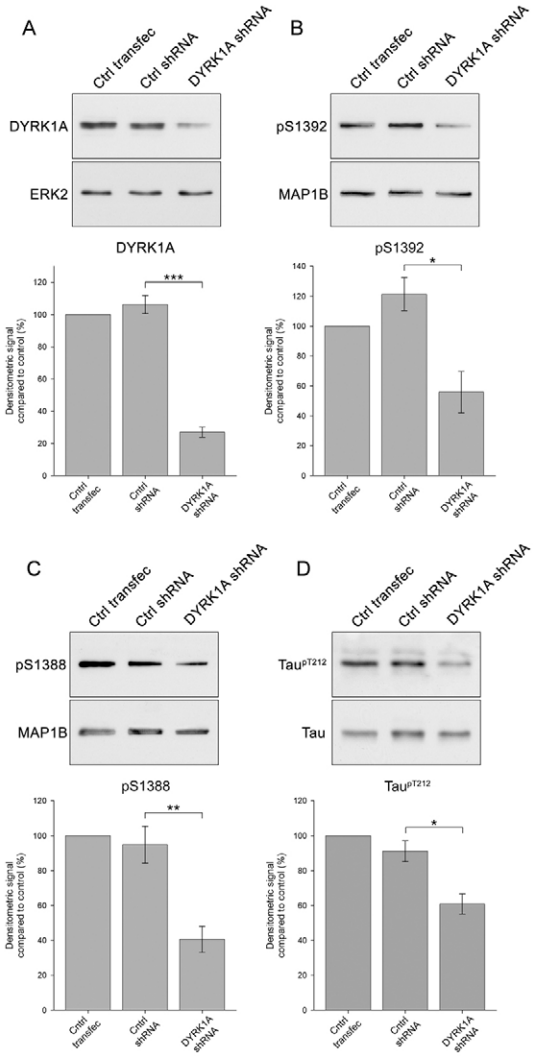

Fig. 6. shRNA knockdown of DYRK1A in cortical neurons reduces MAP1B S1392 and S1388 phosphorylation. Representative immunoblots of samples from cortical cultures transfected with empty shRNA vector alone (Ctrl transfec), or transfected with non-targeting shRNA (Ctrl shRNA) or *DYRK1A* shRNA. Blots were probed with a mAb against DYRK1A (A) or with pAbs against MAP1B S1392-*P* (B), MAP1B S1388-*P* (C) or tau T212-*P* (D). A pAb to ERK2 (ERK2), pAb anti-MAP1B-C1, which recognises all forms of MAP1B (MAP1B) and a pAb against tau (DAKO) were used as loading controls. *DYRK1A* shRNA produces a highly significant knockdown of DYRK1A levels, whereas non-targeting shRNA has no effect. Knockdown of DYRK1A is associated with marked reductions in the phosphorylation of MAP1B S1392 (B), MAP1B S1388 (C) and tau T212 (D). Histograms show quantification of immunoblots from three or more independent experiments. Error bars are s.e.m. for three or more independent experiments. $^{*}P<0.05$, $^{**}P<0.01$, $^{***}P<0.001$.

(Woods et al., 2001; Ryoo et al., 2007; Liu et al., 2008), and so we investigated whether knockdown of DYRK1A was associated with a reduction of phosphorylated tau in cortical neurons using an antibody specific for tau phosphorylated at T212 (tau T212-*P*). This showed that DYRK1A knockdown produces a significant reduction in the levels of tau T212-*P* (Fig. 6D).

Transfection of non-neuronal cells with MAP1B mutated at S1392 partially rescues the loss of stable microtubules

To investigate the role that phosphorylation of S1392 by DYRK1A and the subsequent phosphorylation of S1388 by GSK3β has on microtubule dynamics, we transiently transfected with cDNA encoding full-length MAP1B or the MAP1B mutants S1388A and S1392A into COS-7 cells (Goold et al., 1999; Trivedi et al., 2005). These cells are ideally suited for these experiments because they have only low levels of endogenous MAP1B (Goold et al., 1999). When cDNA encoding full-length MAP1B was transfected into COS-7 cells, it became phosphorylated at S1388 and S1392, as indicated by binding of pAb S1388 and pAb S1392, showing that there is sufficient endogenous kinase activity in COS-7 cells to phosphorylate transfected MAP1B at these sites (Fig. 7A). Immunoblotting with anti-GSK3β and anti-DYRK1A antibodies confirmed the presence of these kinases in COS-7 cells (not shown). However, when COS-7 cells were transfected with cDNA encoding the S1388A point-mutated MAP1B, it became phosphorylated at S1392, albeit at a lower level than in wild-type MAP1B, but not at S1388. By contrast, when COS-7 cells were transfected with cDNA encoding S1392A point-mutated MAP1B, it failed to become phosphorylated at either S1388 or S1392 (Fig. 7A). These findings in transfected COS-7 cells independently support the idea that phosphorylation of S1392 by DYRK1A acts to prime the subsequent phosphorylation of S1388 by GSK3β.

MAP1B influences microtubule dynamics in differentiating neurons and this function is regulated by GSK3β phosphorylation (Goold et al., 1999; Trivedi et al., 2005). When transiently transfected into COS-7 cells, *MAP1B* reduces the number of stable

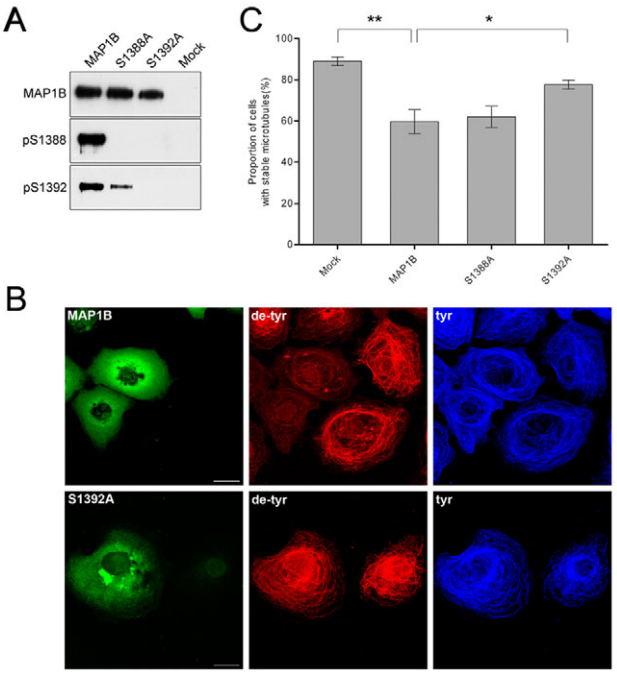

Fig. 7. S1392A point-mutated MAP1B expression in COS-7 cells partially reverses the loss of stable microtubules. (A) Heterologous transfection of cDNA encoding MAP1B, and S1388A and S1392A point-mutated MAP1B confirms that S1392 is a priming site for S1388. COS-7 cells were transiently transfection with cDNA encoding wild-type MAP1B, with MAP1B in which serine 1388 has been mutated to an alanine (S1388A), MAP1B in which serine 1392 has been mutated to an alanine (S1392A) or mock transfected (Mock). Proteins from transfected cells were separated by SDS PAGE and analysed by immunoblotting with pAb N19, which recognises all forms of MAP1B (MAP1B), pAb S1388-*P* (pS1388) or pAb S1392-*P* (pS1392). Transfected S1388A MAP1B is not phosphorylated at S1388 but is phosphorylated at S1392, whereas S1392A MAP1B is not phosphorylated at either S1388 or S1392. (B) Transfection of COS-7 cells with S1392A point-mutated MAP1B partially rescues the loss of stable microtubules. COS-7 cells were transfected with either wild-type MAP1B (MAP1B) or S1392A MAP1B (S1392A) and cells were immunolabelled with an antibody against detyrosinated α-tubulin (de-tyr), which labels stable microtubules, and an antibody against tyrosinated α-tubulin (tyr), which labels unstable microtubules. Expression of wild-type MAP1B is associated with a loss of stable microtubules (de-tyr), whereas cells expressing S1392A MAP1B have a normal population of stable microtubules. Scale bar: 25 μm. (C) Transfection of COS-7 cells with cDNA encoding S1392A point-mutated MAP1B partially rescues the loss of stable microtubules. Histograms showing the proportion of COS-7 cells containing stable microtubules following transfection with either wild-type MAP1B (MAP1B), S1388A MAP1B (S1388A) or S1392A MAP1B (S1392A). Transfection with S1392A MAP1B partially rescues the loss of stable microtubules that is seen with wild-type MAP1B. Cells were scored as lacking stable microtubules if they had no microtubules labelled with an antibody against detyrosinated α-tubulin. Results are mean ± s.e.m. for three, separate experiments in which 100 cells were counted in each experiment. **P*<0.05, ***P*<0.01.

microtubules, an effect that is enhanced when MAP1B is phosphorylated by co-transfection with GSK3β (Goold et al., 1999; Trivedi et al., 2005). Previous experiments have shown that transfection of MAP1B mutated at S1260 and T1265 partially rescues the loss of stable microtubules (Trivedi et al., 2005). To explore the role of phosphorylation of S1388 and S1392 in regulating microtubule dynamics, we transfected cDNA encoding either the S1388A or the S1392A point-mutated MAP1B into COS-7 cells and labelled the cells with antibodies that recognise either stable or unstable microtubules (Trivedi et al., 2005). Transfection of wild-type *MAP1B* into COS-7 cells produced a reduction in the level of stable microtubules but no change in unstable microtubules, as shown previously (Goold et al., 1999; Trivedi et al., 2005). This effect was partially reversed by the S1392A point-mutated MAP1B, but not by the S1388A point-mutated MAP1B, as judged by labelling with antibodies against tyrosinated or detyrosinated α-tubulin, markers for unstable or stable microtubules, respectively (Fig. 7B,C). This finding further supports the idea that DYK1A primes the GSK3β-phosphorylation site at S1388 by phosphorylating S1392 and shows that primed sites affect microtubule stability.

Knockdown of DYRK1A in cortical neurons disrupts neuritogenesis and alters microtubule stability

To further examine a possible regulatory role of DYRK1A phosphorylation of MAP1B on microtubule stability, we tested the effects of DYRK1A knockdown on neuritogenesis in cultured cortical neurons, because this depends on a coordinated regulation of microtubule distribution and dynamics both at the beginning of neurite formation and during neurite extension (Baas, 1999). We examined cultured cortical neurons 2-3 days after transfection with *DYRK1A* shRNA incorporated into a vector that coexpresses the fluorescent protein Venus, to identify transfected cells (Fig. 8A). We found that neuritogenesis was disrupted to varying degrees following transfection with *DYRK1A* shRNA. In most cases, neurons produced abnormally short neurites that were often highly branched (Fig. 8A). Compared with neurons transfected with a non-targeting shRNA-Venus vector, neurons transfected with *DYRK1A*-shRNA–Venus extended neurites that were 30% shorter (Fig. 8C) and had up to 2.20 branches per neurite compared with 1.55 branches per neurite in control cultures (Fig. 8D). The average number of primary neurites per neuron, however, did not change (not shown). Embryonic cortical neurons polarise in culture to produce one axon and several dendrites (Ledesma and Dotti, 2003). To determine whether *DYRK1A*-shRNA–Venus transfection of neurons affected neuronal polarity, as well as neuritogenesis, we immunolabelled transfected cortical cultures with antibodies against dendritic (MAP2) and axonal (tau-1) markers (Fig. 8B), and determined the proportion of transfected neurons with tau-1- or MAP2-positive neurites. This showed that neurons transfected with non-targeting shRNA had MAP2-positive/tau-1-negative cell bodies and that all neurites were MAP2-positive/tau-1-negative along their entire length except the longest neurite, which was MAP2-positive proximally and tau-1-positive distally. Non-transfected neurons had a similar labelling pattern. Neurons transfected with *DYRK1A* shRNA also had MAP2-positive/tau-1-negative cell bodies and minor neurites (Fig. 8B), but the proportion of neurons that had tau-1-positive neurites was reduced by 50% (Fig. 8E). This suggests that knockdown of DYRK1A does not block neuronal polarity but slows down its acquisition, probably by retarding axonogenesis.

The COS-7 transfection experiments described above suggest that DYRK1A phosphorylation of MAP1B is involved in microtubule dynamics and predicts that knockdown of DYRK1A in neurons would increase the number of stable microtubules. To test this idea, we probed immunoblots of *DYRK1A*-shRNA-transfected neurons with an antibody that recognises detyrosinated α-tubulin, a marker for stable microtubules (Fig. 9). Unexpectedly, this showed that DYRK1A knockdown is associated with a decrease in detyrosinated α-tubulin (Fig. 9). One explanation for the discrepancy between this result and that in COS-7 cells (Fig. 7) is the presence of

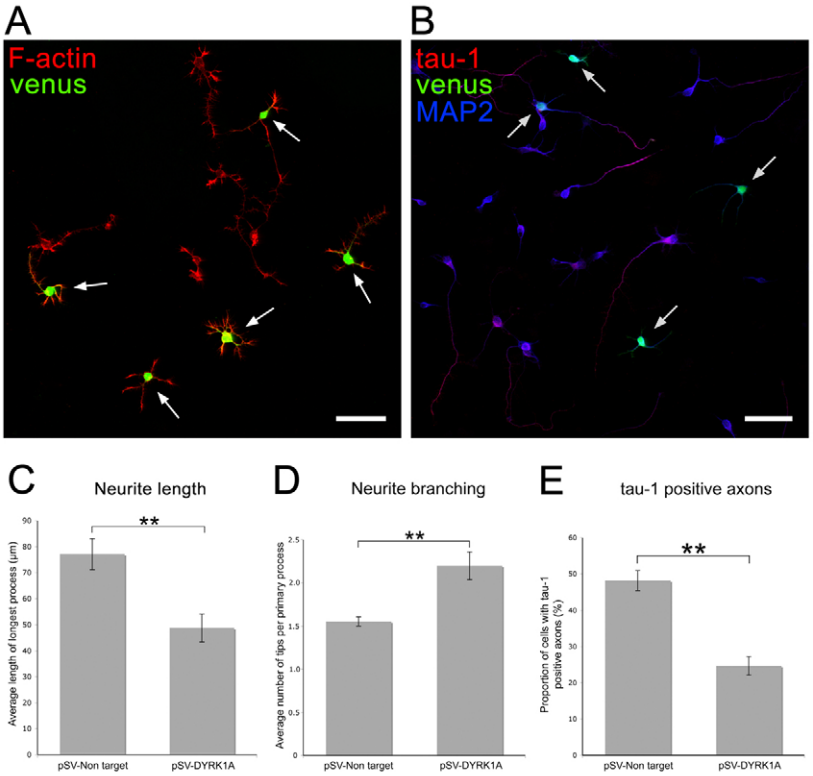

Fig. 8. shRNA knockdown of DYRK1A in cortical neurons compromises neuritogenesis. (A) Cortical cultures were transfected with *DYRK1A*-shRNA–Venus (venus) to knock down DYRK1A, and, to visualise neuronal processes, cultures were labelled with phalloidin, which binds to actin filaments (F-actin). Transfected neurons, identified by the expression of the Venus protein (arrows), extend neurites that are on average shorter and more highly branched than the neurites of non-transfected neurons. Scale bars: 25 μm. (B) Cortical cultures were transfected with *DYRK1A*-shRNA–Venus (venus), to knock down DYRK1A, and immunolabelled with antibodies to tau-1, to label axons (tau-1), and to MAP2, to label cell bodies and dendrites (MAP2). Fewer transfected cells (arrows) have tau-1-positive axons than non-transfected cells. (C-E) Histograms showing the average length of the longest process (C), the degree of process branching (D) and the proportion of neurons with tau-1-positive axons (E) of neurons transfected with either a pSuperVenus vector containing a non-targeting shRNA sequence (pSV-Non target) or with pSuperVenus-*DYRK1A* shRNA (pSV-DYRK1A). Neurons in which DYRK1A has been knocked down have shorter neurites, a higher degree of neurite branching and fewer axons. Results are mean ± s.e.m. for five separate experiments in which 75 or more neurons were counted in each experiment. $^{**}P<0.008$ (C), $^{**}P<0.005$ (D), $^{**}P<0.001$ (E).

DYRK1A substrates other than MAP1B in neurons, such as tau (Woods et al., 2001). To test for a role of tau in microtubule dynamics, we looked at the effects of knockdown of tau on detyrosinated α-tubulin levels. When tau was knocked down in cortical neurons using siRNA, there was no effect on the levels of detyrosinated α-tubulin (Fig. 9). However, when DYRK1A and tau were knocked down simultaneously, the reduction in the levels of detyrosinated α-tubulin seen with DYRK1A knockdown alone was reversed (Fig. 9A,B).

Discussion

DYRK1A primes the GSK3β phosphorylation of MAP1B at S1388

We found evidence that DYRK1A phosphorylates S1392 on MAP1B and that this primes the phosphorylation of S1388 by GSK3β. Our evidence includes the observation that inhibition of DYRK1A, either with pharmacological inhibitors (purvalanol and EGCG) or by shRNA knockdown, reduced S1392 phosphorylation. Unexpectedly, pharmacological inhibition of DRYK1A was associated with an increase in S1388 phosphorylation, whereas a decrease is predicted if phosphorylation of S1392 primes phosphorylation of S1388. However, independent evidence from shRNA knockdown of DYRK1A clearly showed that S1392 is a priming site for GSK3β phosphorylation of S1388 in MAP1B. Although we do not know the explanation for the increase in S1388 phosphorylation when DYRK1A is inhibited with pharmacological inhibitors, it might represent a side-effect of the compounds used to inhibit DYRK1A, e.g. inhibition of a S1388 phosphatase. Further evidence that DYRK1A phosphorylation of S1392 primes GSK3β phosphorylation of S1388 came from analysis of the phosphorylation of full-length MAP1B in vivo that was mutated at either S1388 or S1392. As predicted, mutating S1392 so that it cannot be phosphorylated abolished the phosphorylation of S1388. DYRK1A and DYRK2 have been shown to prime a GSK3β-phosphorylation site on the microtubule-associated protein tau (Woods et al., 2001; Liu et al., 2008), and DYRK2 primes a GSK3β-phosphorylation site on CRMP4 (Cole et al., 2006). Thus, DYRKs are emerging as common priming kinases for substrates that are phosphorylated by GSK3β in growing axons and growth cones.

DYRK1A is a proline-directed serine/threonine kinase that is highly expressed in the developing nervous system (Okui et al., 1999), but its function in neural development is unclear. In humans, *DYRK1A* maps to the Down's syndrome (DS) critical region on chromosome 21 and is a candidate gene responsible for mental retardation and Alzheimer's disease in DS patients. Consistent with this, DYRK1A mRNA and protein are overexpressed in DS brains (Guimera et al., 1999; Liu et al., 2008) and transgenic mice overexpressing human DYRK1A exhibit a phenotype reminiscent of that seen in DS patients, such as cognitive deficits and tau hyperphosphorylation (Altafaj et al., 2001; Ahn et al., 2006; Ryoo et al., 2007). DYRK1A-knockout mice die in utero and, although heterozygotes can survive to adulthood, they have reduced neuronal numbers (Fotaki et al., 2002). Loss-of-function of the *Drosophila* orthologue Minibrain is associated with a marked reduction in the size of the optic lobes and central hemispheres in the adult brain (Tejedor et al., 1995), suggesting that Minibrain, and therefore also DYRK1A, is a regulator of neuronal-cell proliferation or differentiation. Support for a role of DYRK1A in neuronal differentiation comes from experiments with immortalised hippocampal-progenitor cells that show that overexpression of a kinase-deficient DYRK1A mutant in these cells attenuates their differentiation (Yang et al., 2001), and from the observation that overexpression of DYRK1A potentiates nerve growth factor (NGF)-driven differentiation of PC12 cells (Kelly and Rahmani, 2005).

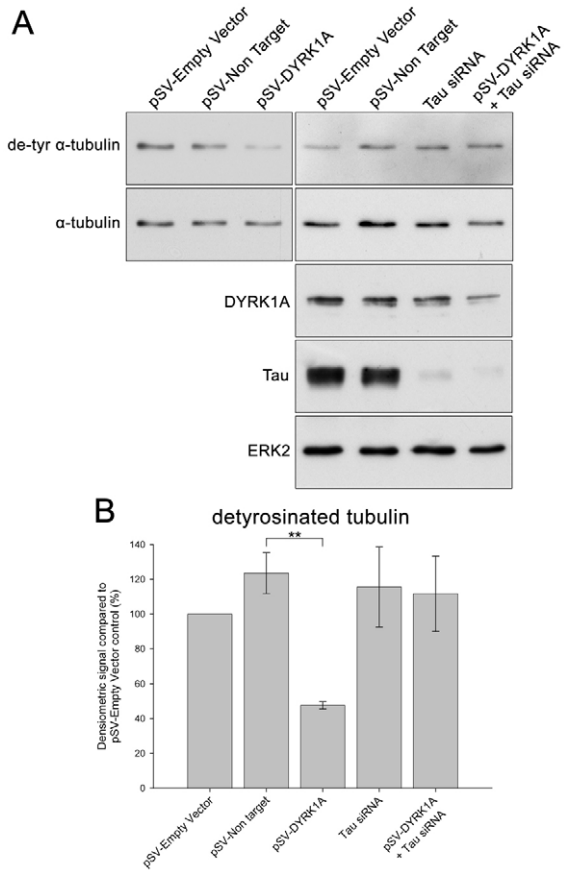

Fig. 9. shRNA knockdown of DYRK1A in cortical neurons alters microtubule dynamics. (A) Representative immunoblots of samples from cortical cultures transfected with an empty pSuperVenus vector (pSV-Empty Vector), a pSuperVenus vector containing a non-targeting shRNA sequence (pSV-Non target), pSuperVenus–*DYRK1A*-shRNA (pSV-DYRK1A) or with *tau* siRNA. Blots were probed with antibodies against detyrosinated α-tubulin (de-tyr α-tubulin), as a marker for stable microtubules, all forms of α-tubulin (α-tubulin), and DYRK1A, tau or ERK2. Knockdown of DYRK1A is associated with a reduction in the levels of detyrosinated α-tubulin, an effect that is reversed by simultaneous knockdown of tau. (B) Histogram showing the relative proportion of α-tubulin that is detyrosinated in samples from cortical cultures transfected with an empty pSuperVenus vector, a pSuperVenus vector containing a non-targeting shRNA sequence, with pSuperVenus–*DYRK1A*-shRNA or with tau siRNA. Immunoblots were quantified by densitometry. Results are mean ± s.e.m. for three separate experiments. $^{**}P<0.002$.

In embryonic rat spinal cord, GSK3β-phosphorylated MAP1B is restricted to neuronal-cell bodies and growing axons

We chose to examine phosphorylated MAP1B expression in the developing spinal cord because the development of the spinal cord is extensively documented in rodents and the trajectories of growing axons are well defined. MAP1B and GSK3β are distributed throughout the somato-dendritic and axonal compartments of differentiating neurons in the developing spinal cord (Trivedi et al., 2005). However, despite this ubiquitous distribution, we found, in a previous study, that two nonprimed GSK3β-phosphorylation sites on mouse MAP1B, S1260 and T1265 (S1256 and T1261 in rat), recognised by polyclonal antibodies BUGS and SuperBUGS, respectively (Trivedi et al., 2005), were exclusively expressed in growing axons of embryonic neurons. Furthermore, this axonal distribution, particularly for SuperBUGS, is in the form of a gradient that is highest distally (Fig. 3). In the present work, we confirmed these findings and, in addition, showed that a primed MAP1B GSK3β-phosphorylation site at S1388 and its priming site, S1392, are also expressed in growing axons but uniformly along their length, and, in addition, are present in neuronal-cell bodies of embryonic neurons. This difference in the distribution of primed and nonprimed GSK3β-phosphorylation sites in MAP1B suggests that there is a differential regulation of primed and nonprimed sites in differentiating neurons, and indeed there is evidence that primed and nonprimed GSK3β sites have different roles in axonal differentiation (Kim et al., 2006).

Microtubule stability is regulated by both primed and nonprimed GSK3β-phosphorylation sites on MAP1B

We have shown previously that expression of GSK3β-phosphorylated MAP1B in COS-7 cells results in the loss of stable microtubules from these cells, implying that GSK3β-phosphorylated MAP1B regulates microtubule stability (Goold et al., 1999). There is also evidence that phosphorylation of MAP1B by GSK3β regulates the control of microtubule dynamics that MAP1B exerts in growing axons and growth cones (Goold et al., 1999; Owen and Gordon-Weeks, 2003) (see also Kawauchi et al., 2005). Identifying GSK3β sites in MAP1B provided the opportunity to test the role of these sites in regulating MAP1B function. Previously, we found that point-mutated MAP1B, in which serine 1260, threonine 1265 or both were changed to a valine, so that they could not be phosphorylated by GSK3β at these sites, only partially rescued the loss of stable microtubules that GSK3β-phosphorylated MAP1B causes when cDNA encoding it is transfected into non-neuronal cells (Trivedi et al., 2005). As well as confirming that GSK3β sites on MAP1B are involved in the regulation of microtubule dynamics, this finding suggests that other MAP1B GSK3β sites also contribute to the regulation of microtubule stability. In the present paper, we identified a primed GSK3β site on MAP1B and provided evidence that it is also involved in the regulation of microtubule stability. Furthermore, point-mutation analysis showed that phosphorylation of S1388 is insufficient for regulating microtubule stability, because S1392 must also be phosphorylated. Thus, both primed and nonprimed GSK3β sites on MAP1B regulate microtubule dynamics.

Knockdown of DYRK1A in cortical neurons disrupts neuritogenesis and alters microtubule stability

Knockdown of DYRK1A in cultured embryonic cortical neurons disrupted neuritogenesis; neurons produced shorter and more highly branched neurites, and fewer neurons developed axons. This differentiation phenotype is reminiscent of that seen when primed GSK3β sites are differentially inhibited by low concentrations of GSK3 inhibitors (Kim et al., 2006). By contrast, when both primed and nonprimed GSK3β sites are inhibited, using high concentrations of GSK3 inhibitors, neurons produce shorter and thicker neurites that end in abnormally large growth cones (Lucas et al., 1998; Goold et al., 1999; Kim et al., 2006), a phenotype not seen with DYRK1A knockdown. These observations suggest that primed GSK3β sites are important in axonogenesis, probably by regulating microtubule dynamics. However, when we examined the effect of inhibiting DYRK1A activity on microtubule dynamics, we obtained opposing results. Mutation of the site of DYRK1A phosphorylation on MAP1B partially reduced the decrease in stable microtubules that GSK3β phosphorylation of MAP1B produces in transfected COS-7 cells, whereas knockdown of DYRK1A in embryonic cortical neurons decreased the proportion of detyrosinated α-tubulin, a

marker for stable microtubules. This discrepancy is probably due to contributions from DYRK1A substrates other than MAP1B in neurons, such as tau (Woods et al., 2001), that are not present in COS-7 cells. Consistent with this idea, we found that DYRK1A knockdown reduced phosphorylation of tau T212, a site of DYRK1A phosphorylation, in cortical neurons. Furthermore, knockdown of tau in cortical neurons blocked the effect of knockdown of DYRK1A on the levels of detyrosinated α-tubulin. These results suggest that DYRK1A phosphorylation of tau and MAP1B have reciprocal effects on the level of detyrosinated α-tubulin in cortical neurons, and underscores the idea that neuritogenesis depends on a balance between opposing effects on microtubule dynamics in differentiating neurons (Goold and Gordon-Weeks, 2004).

Materials and Methods

Materials

B27 serum-free supplement, D-glucose, DMEM, foetal bovine serum, Hank's Balanced Salt Solution, HEPES, Lipofectamine 2000 and sodium pyruvate were purchased from Invitrogen. Neurobasal medium without glutamine was from Invitrogen Life Technologies and Papain Dissociation Kit from Worthington. DMAT, purvalanol and SP600125 were from Calbiochem, and all other chemicals were purchased from Sigma.

Purification of MAP1B

MAP1B was partially purified from neonatal (day 5) rat brain by dissociating MAP1B from taxol-stabilised microtubules using poly-L-aspartic acid (Johnstone et al., 1997). Phosphatase and protease inhibitors (Pierce) were used throughout. Proteins were separated by one-dimensional SDS polyacrylamide gel electrophoresis on a 6% acrylamide minigel (BioRad). Following Coomassie blue staining (Pierce), bands were excised from gels, digested with Asp-N, chymotrypsin or trypsin and analysed by tandem mass spectrometry using a Z-spray source fitted to a QTof-micro (Micromass, UK) (Proteome Sciences, Institute of Psychiatry, King's College London).

Cloning of full-length *GFP-MAP1B* and generation of point mutations at S1388 and S1392

Full-length MAP1B fused to the green fluorescent protein (GFP) at the N-terminus (GFP-MAP1B) was produced by PCR amplification of mouse *MAP1B* cloned into the pSVsport vector (Noble et al., 1989). The primers were: forward, 5′-TATGTCGACATGGCGACCGTGGTGGTG-3′; reverse, 5′-TCGCCCGGG-CTACAGTTCTATCTTGCATGC-3′. The PCR products were subcloned into pEGFP-C1 (Invitrogen).

Oligonucleotide-directed mutagenesis was used in conjunction with PCR and cloning to introduce point mutations into the *MAP1B* sequence in the GFP vector. Point mutations were introduced at residues S1388 and S1392, exchanging the serine for an alanine using the QuikChange XL Site-Directed Mutagenesis Kit (Stratagene). The primers were: S1388A forward, 5′-TGTGGAGAAGGTTCTGG-CTCCTTTACGCAGTCC-3′; S1388A reverse, 5′-GGACTGCGTAAAGGAGCC-AGAACCTTCTCCACA-3′; S1392A forward, 5′-GTTCTGTCTCCTTTACG-CGCTCCTCCCCTTCTTGGATC-3′; S1392A reverse, 5′-GATCCAAGA-AGGGGAGGAGCGCGTAAAGGAGACAGAAC-3′. Clones were verified by restriction digest and direct sequencing (Dundee University Sequencing Service).

Culture, transfection and immunofluorescence microscopy of COS-7 cells

COS-7 cells were cultured and transiently transfected with either full-length mouse *GFP-MAP1B* cDNA (wild-type MAP1B) or point-mutated *GFP-MAP1B* (either S1388A or S1392A) as described previously (Goold et al., 1999). Cells were transfected using Lipofectamine 2000 reagent and 2 μg DNA per dish according to the manufacturer's protocol. For controls, cells were treated as for transfections except that DNA was omitted (mock transfection). At 24 hours after transfection, the cells were either harvested for immunoblotting by washing twice with phosphate buffered saline (PBS) and solubilising in 300 μl SDS sample buffer or fixed for immunofluorescence. For fixation, cells were washed twice with PBS at 37°C and fixed for 10 minutes with 3% formaldehyde, 0.2% glutaraldehyde and 0.2% Triton X-100 in PHEM buffer at 37°C (Schliwa and van Blerkom, 1981). Fixed cultures were treated with blocking buffer [BB; 5% (v/v) normal horse serum, 5% (v/v) normal goat serum, 50 mM L-lysine and 0.2% (v/v) Triton X-100 in PBS] and were then incubated with antibodies to tyrosinated α-tubulin (YL 1/2, Sera Lab, 1:50) and detyrosinated α-tubulin (Chemicon, 1:500) diluted in BB followed by the appropriate Alexa-Fluor-conjugated secondary antibodies (Molecular Probes) diluted in BB. Finally, cultures were washed with PBS and mounted onto microscope slides in FluorSave (Calbiochem) and viewed under a Leica TCS confocal microscope.

Protein-kinase assay

An in vitro protein-kinase assay was used essentially as described previously (Johnstone et al., 1997; Lucas et al., 1998). Briefly, the GST-MAP1B fusion protein, SP, encoding mouse MAP1B amino acids 1244-1530 [1240-1526 in rat (Trivedi et al., 2005)] bound to GSH-linked agarose beads was incubated for various times at room temperature with a high-speed supernatant from neonatal rat brain in kinase buffer.

pAb production

The production of pAb BUGS and pAb SuperBUGS has been described (Trivedi et al., 2005). For the production of additional phosphorylation-dependent antibodies, two synthetic phospho-peptides, corresponding to amino acids 1384-1395 of rat MAP1B, in which either S1388 or S1392 were phosphorylated (CKVLSPLRSPPL; phosphorylated amino acids underlined), were synthesised and conjugated to keyhole limpet haemocyanin. Anti-sera pAb S1388-*P* and pAb S1392-*P* were raised in rabbits (Eurogentec, Herstal, Belgium). Unphosphorylated peptides, of the same sequence, were also synthesised for column chromatography and peptide-inhibition studies (see below) (Eurogentec). Anti-sera were immuno-affinity purified using Pierce Sulfolink kits (Perbio Science UK, Cramlington, UK), first on phospho-peptide columns and then on non-phospho-peptide columns, to separate non-phospho-specific antibodies.

Phospho-specificity assays

Antibodies were tested for phospho-specificity using two assays: phospho-peptide inhibition and in vitro protein-kinase assays. For the phospho-peptide inhibition assay, antibodies were pre-incubated at room temperature for 1 hour with the appropriate non-phosphorylated or phosphorylated peptides (0.8 μM or 8 μM) before testing in immunoblots against a neonatal rat brain extract. In vitro protein-kinase assays using recombinant MAP1B proteins are described above.

Gel electrophoresis and immunoblotting

Electrophoresis and immunoblotting were done as described previously (Goold and Gordon-Weeks, 2005). The following antibodies were used: pAb N19 (Santa Cruz Biotechnology; 1:4000), pAb anti-MAP1B-C1, which recognise all forms of MAP1B [(Johnstone et al., 1997) 1:100,000], pAb BUGS (1:5000) and pAb SuperBUGS (1:3000), which recognise GSK3β-phosphorylated MAP1B (Trivedi et al., 2005), monoclonal antibody (mAb) AC-15, which recognises β-actin (Sigma; 1:10,000), mAb DM1A (Sigma), which recognises α-tubulin, pAb Glu-tub (Chemicon), which recognises detyrosinated α-tubulin, a pAb against GST (Abcam; 1:30,000), pAb Tau phospho-T212 (Abcam; 1:5000) and pAb anti-Tau (Dako; 1:100,000). pAbs S1388-*P* and S1392-*P* were used in western blots at 1:2000. Western blots are representative of at least three independent experiments. Immunoblots were quantified as described previously using Phoretix 1D Plus software (Goold et al., 1999).

Preparation of tissue for immunostaining

Wistar rat pregnancies were dated by counting the day of a vaginal plug as embryonic (E) day 0. E12 rat embryos were dissected out of pregnant females anaesthetised with an intraperitoneal injection of sodium pentobarbitone (Sagatal) and, after decapitation, fixed by immersion for 2 hours in a solution of 3% (w/v) formaldehyde and 0.2% (v/v) glutaraldehyde in PBS at 37°C.

Immunostaining of tissue sections

Immunostaining of spinal-cord sections was as described previously (Trivedi et al., 2005). Immunolabelling was performed by incubating sections overnight at 4°C with pAb BUGS (1:200), pAb SuperBUGS (1:900), phosphospecific pAbs S1388-*P* (1:200) and S1392-*P* (1:300), and pAb MAP1B (N19) against all forms of MAP1B (1:1000; Santa Cruz Biotechnology) diluted in BB, followed by a peroxidase-conjugated goat anti-rabbit or rabbit anti-goat antibody diluted in BB (1:100; DAKO) for 2 hours. Sections were extensively washed between each step with PBS and the antibody complex was visualised with diaminobenzidine (Sigma) at 0.5 mg/ml in Tris-buffered saline containing 0.01% H_2O_2. Controls, in which the primary antibody was replaced with BB, were developed in parallel, and were negative. After washing with PBS, the sections were mounted onto microscope slides in DPX. All sections were viewed with an Olympus BH2 microscope equipped with Nomarski optics and images captured with a DP70 colour CCD camera (Olympus).

Culture and immunofluorescent microscopy of cerebral cortical neurons

Cerebral cortices were dissected from day 17-18 rat embryos in Hank's balanced salt solution and dissociated using papain (Worthington) followed by trituration with a pipette. Cells (8×10^5) were plated in six-well plates (Nunc) coated with poly-D-lysine (100 μg/ml, Sigma) and laminin (20 μg/ml, Sigma). Cells were incubated at 37°C in 5% CO_2 in humidified air in Neurobasal medium supplemented with 2% (v/v) B27 supplement, 2 mM glutamine/100 I.U./ml penicillin/100 I.U./ml streptomycin and 0.45% D-(+) glucose.

The following kinase inhibitors were added to cortical cultures: EGCG (50 μM), lithium chloride (20 mM), purvalanol (10 μM), roscovitine (20 μM,), SP600125 (10 μM) or 4-benzyl-2-methyl-1,2,4-thiadiazolidine-3,5-dione (TDZD-8, 5 mM) after 3 days in culture and left for 3 hours, after which cultures were harvested for immunoblot analysis (Goold and Gordon-Weeks, 2005). Sodium chloride (20 mM) or dimethyl sulphoxide (0.2%) were used as controls where appropriate.

Cortical cultures to be used for immunofluorescence were processed as described for COS-7 cells, with the exception that neurons were fixed with 3% formaldehyde and 0.2% glutaraldehyde in PBS. Neurons were labelled with the following primary antibodies: tau-1 (Millipore, 1:250) and MAP2 (AB5622, Millipore, 1:50).

Knockdown of DYRK1A and tau in cerebral cortical neurons

To identify shRNA sequences that could knockdown *DYRK1A* in cortical neurons, we screened five MISSION shRNA clones (Sigma) targeted against the mouse *DYRK1A* sequence (NCBI no. NM_007890). The effect of the shRNA clones on DYRK1A protein levels in rat cortical neurons was assayed by immunoblotting using anti-DYRK1A mAb clone 7D10 (Abnova). The clone that resulted in the greatest knockdown of DYRK1A was selected (targeting sequence 5′-CGATGGCACTTGGAGCTTAAA-3′), and a clone that gave no significant knockdown of DYRK1A (targeting sequence 5′-CGGTATGAAATCGACTCCTTA-3′) was used as a control.

The shRNA targeting sequence that gave the greatest knockdown of DYRK1A was also cloned into a vector (pSuperVenus) based on pSuper (OligoEngine), into which a cassette containing the coding sequence for Venus fluorescent protein and a CMV promoter had been inserted (Kim et al., 2006). The *DYRK1A* shRNA targeting sequence and the MISSION non-targeting shRNA control sequence (Sigma) were inserted into pSuperVenus at the *Bgl*II-*Hind*III sites using oligonucleotides constructed according to the method detailed in the pSuper manual.

shRNA plasmids were purified using endotoxin-free Maxi-Prep kits (Qiagen) and transfected into E17 rat cortical neurons at the time of plating by nucleofection using an Amaxa rat nucleofection kit (program O-03).

For tau knockdown, four different siRNA duplexes were used (Dharmacon SMARTpool, accession number NM-017212) as described previously (Qiang et al., 2006).

The Wellcome Trust and the MRC funded this work. S.L. was supported by an MRC postgraduate studentship. Bill Snider kindly provided the pSuperVenus vector and Diane Hanger the phospho-tau antibodies. Deposited in PMC for release after 6 months.

References

Ahn, K. J., Jeong, H. K., Choi, H. S., Ryoo, S. R., Kim, Y. J., Goo, J. S., Choi, S. Y., Han, J. S., Ha, I. and Song, W. J. (2006). DYRK1A BAC transgenic mice show altered synaptic plasticity with learning and memory defects. *Neurobiol. Dis.* **22**, 463-472.

Allen, E., Ding, J., Wang, W., Pramanik, S., Chou, J., Yau, V. and Yang, Y. (2005). Gigaxonin-controlled degradation of MAP1B light chain is critical to neuronal survival. *Nature* **438**, 224-228.

Altafaj, X., Dierssen, M., Baamonde, C., Marti, E., Visa, J., Guimera, J., Oset, M., Gonzalez, J. R., Florez, J., Fillat, C. et al. (2001). Neurodevelopmental delay, motor abnormalities and cognitive deficits in transgenic mice overexpressing Dyrk1A (minibrain), a murine model of Down's syndrome. *Hum. Mol. Genet.* **10**, 1915-1923.

Baas, P. W. (1999). Microtubules and neuronal polarity: lessons from mitosis. *Neuron* **22**, 23-31.

Bain, J., McLauchlan, H., Elliott, M. and Cohen, P. (2003). The specificities of protein kinase inhibitors: an update. *Biochem. J.* **371**, 199-204.

Ballif, B. A., Villen, J., Beausoleil, S. A., Schwartz, D. and Gygi, S. P. (2004). Phosphoproteomic analysis of the developing mouse brain. *Mol. Cell Proteomics* **3**, 1093-1101.

Bennett, B. L., Sasaki, D. T., Murray, B. W., O'Leary, E. C., Sakata, S. T., Xu, W., Leisten, J. C., Motiwala, A., Pierce, S., Satoh, Y. et al. (2001). SP600125, an anthrapyrazolone inhibitor of Jun N-terminal kinase. *Proc. Natl. Acad. Sci. USA* **98**, 13681-13686.

Chang, L., Jones, Y., Ellisman, M. H., Goldstein, L. S. and Karin, M. (2003). JNK1 is required for maintenance of neuronal microtubules and controls phosphorylation of microtubule-associated proteins. *Dev. Cell* **4**, 521-533.

Ciani, L., Krylova, O., Smalley, M. J., Dale, T. C. and Salinas, P. C. (2004). A divergent canonical WNT-signaling pathway regulates microtubule dynamics: dishevelled signals locally to stabilize microtubules. *J. Cell Biol.* **164**, 243-253.

Cole, A. R., Causeret, F., Yadirgi, G., Hastie, C. J., McLauchlan, H., McManus, E. J., Hernandez, F., Eickholt, B. J., Nikolic, M. and Sutherland, C. (2006). Distinct priming kinases contribute to differential regulation of collapsin response mediator proteins by glycogen synthase kinase-3 *in vivo*. *J. Biol. Chem.* **281**, 16591-16598.

Collins, M. O., Yu, L., Coba, M. P., Husi, H., Campuzano, I., Blackstock, W. P., Choudhary, J. S. and Grant, S. G. (2005). Proteomic analysis of *in vivo* phosphorylated synaptic proteins. *J. Biol. Chem.* **280**, 5972-5982.

Del Rio, J. A., Gonzalez-Billault, C., Urena, J. M., Jimenez, E. M., Barallobre, M. J., Pascual, M., Pujadas, L., Simo, S., La, T. A., Wandosell, F. et al. (2004). MAP1B is required for Netrin 1 signaling in neuronal migration and axonal guidance. *Curr. Biol.* **14**, 840-850.

DiTella, M. C., Feiguin, F., Carri, N., Kosik, K. S. and Caceres, A. (1996). MAP-1B/TAU functional redundancy during laminin-enhanced axonal growth. *J. Cell Sci.* **109**, 467-477.

Díaz-Nido, J., Serrano, L., Mendez, E. and Avila, J. (1988). A casein kinase II-related activity is involved in phosphorylation of microtubule-associated protein MAP-1B during neuroblastoma cell differentiation. *J. Cell Biol.* **106**, 2057-2065.

Doble, B. W. and Woodgett, J. R. (2003). GSK-3: tricks of the trade for a multi-tasking kinase. *J. Cell Sci.* **116**, 1175-1186.

Fotaki, V., Dierssen, M., Alcantara, S., Martinez, S., Marti, E., Casas, C., Visa, J., Soriano, E., Estivill, X. and Arbones, M. L. (2002). Dyrk1A haploinsufficiency affects viability and causes developmental delay and abnormal brain morphology in mice. *Mol. Cell. Biol.* **22**, 6636-6647.

Gonzalez-Billault, C. and Avila, J. (2000). Molecular genetic approaches to microtubule-associated protein function. *Histol. Histopathol.* **15**, 1177-1183.

Gonzalez-Billault, C., Jimenez-Mateos, E. M., Caceres, A., Diaz-Nido, J., Wandosell, F. and Avila, J. (2004). Microtubule-associated protein 1B function during normal development, regeneration, and pathological conditions in the nervous system. *J. Neurobiol.* **58**, 48-59.

Gonzalez-Billault, C., Del Rio, J. A., Urena, J. M., Jimenez-Mateos, E. M., Barallobre, M. J., Pascual, M., Pujadas, L., Simo, S., Torre, A. L., Gavin, R. et al. (2005). A role of MAP1B in Reelin-dependent neuronal migration. *Cereb. Cortex* **15**, 1134-1145.

Goold, R. G. and Gordon-Weeks, P. R. (2001). Microtubule-associated protein 1B phosphorylation by glycogen synthase kinase 3β is induced during PC12 cell differentiation. *J. Cell Sci.* **114**, 4273-4284.

Goold, R. G. and Gordon-Weeks, P. R. (2003). NGF activates the phosphorylation of MAP1B by GSK3β through the TrkA receptor and not $p75^{NTR}$. *J. Neurochem.* **87**, 935-946.

Goold, R. G. and Gordon-Weeks, P. R. (2004). Glycogen synthase kinase 3β and the regulation of axon growth. *Biochem. Soc. Trans.* **32**, 809-811.

Goold, R. G. and Gordon-Weeks, P. R. (2005). The MAP kinase pathway is upstream of the activation of GSK3β that enables it to phosphorylate MAP1B and contributes to the stimulation of axon growth. *Mol. Cell Neurosci.* **28**, 524-534.

Goold, R. G., Owen, R. and Gordon-Weeks, P. R. (1999). Glycogen synthase kinase 3β phosphorylation of microtubule-associated protein 1B regulates the stability of microtubules in growth cones. *J. Cell Sci.* **112**, 3373-3384.

Gordon-Weeks, P. R. and Fischer, I. (2000). MAP1B expression and microtubule stability in growing and regenerating axons. *Microsc. Res. Tech.* **48**, 63-74.

Guimera, J., Casas, C., Estivill, X. and Pritchard, M. (1999). Human minibrain homologue (MNBH/DYRK1): characterization, alternative splicing, differential tissue expression, and overexpression in Down syndrome. *Genomics* **57**, 407-418.

Hahn, C. M., Kleinholz, H., Koester, M. P., Grieser, S., Thelen, K. and Pollerberg, G. E. (2005). Role of cyclin-dependent kinase 5 and its activator P35 in local axon and growth cone stabilization. *Neuroscience* **134**, 449-465.

Halpain, S. and Dehmelt, L. (2006). The MAP1 family of microtubule-associated proteins. *Genome Biol.* **7**, 224.

Hammarback, J. A., Obar, R. A., Hughes, S. M. and Vallee, R. B. (1991). MAP1B is encoded as a polyprotein that is processed to form a complex N-terminal microtubule-binding domain. *Neuron* **7**, 129-139.

Hanley, J. G., Koulen, P., Bedford, F., Gordon-Weeks, P. R. and Moss, S. J. (1999). The protein MAP-1B links GABA(C) receptors to the cytoskeleton at retinal synapses. *Nature* **397**, 66-69.

Johnstone, M., Goold, R. G., Bei, D., Fischer, I. and Gordon-Weeks, P. R. (1997). Localisation of microtubule-associated protein 1B phosphorylation sites recognised by monoclonal antibody SMI-31. *J. Neurochem.* **69**, 1417-1424.

Kawauchi, T., Chihama, K., Nabeshima, Y. and Hoshino, M. (2003). The in vivo roles of STEF/Tiam1, Rac1 and JNK in cortical neuronal migration. *EMBO J.* **22**, 4190-4201.

Kawauchi, T., Chihama, K., Nishimura, Y. V., Nabeshima, Y. and Hoshino, M. (2005). MAP1B phosphorylation is differentially regulated by Cdk5/p35, Cdk5/p25, and JNK. *Biochem. Biophys. Res. Commun.* **331**, 50-55.

Kelly, P. A. and Rahmani, Z. (2005). DYRK1A enhances the mitogen-activated protein kinase cascade in PC12 cells by forming a complex with Ras, B-Raf, and MEK1. *Mol. Biol. Cell* **16**, 3562-3573.

Kim, W. Y., Zhou, F. Q., Zhou, J., Yokota, Y., Wang, Y. M., Yoshimura, T., Kaibuchi, K., Woodgett, J. R., Anton, E. S. and Snider, W. D. (2006). Essential roles for GSK-3s and GSK-3-primed substrates in neurotrophin-induced and hippocampal axon growth. *Neuron* **52**, 981-996.

Klein, P. S. and Melton, D. A. (1996). A molecular mechanism for the effect of lithium on development. *Proc. Natl. Acad. Sci. USA* **93**, 8455-8459.

Ledesma, M. D. and Dotti, C. G. (2003). Membrane and cytoskeleton dynamics during axonal elongation and stabilization. *Int. Rev. Cytol.* **227**, 183-219.

Liu, F., Liang, Z., Wegiel, J., Hwang, Y. W., Iqbal, K., Grundke-Iqbal, I., Ramakrishna, N. and Gong, C. X. (2008). Overexpression of Dyrk1A contributes to neurofibrillary degeneration in Down syndrome. *FASEB J.* **22**, 3224-3233.

Lu, R., Wang, H., Liang, Z., Ku, L., O'donnell, W. T., Li, W., Warren, S. T. and Feng, Y. (2004). The fragile X protein controls microtubule-associated protein 1B translation and microtubule stability in brain neuron development. *Proc. Natl. Acad. Sci. USA* **101**, 15201-15206.

Lucas, F. R., Goold, R. G., Gordon-Weeks, P. R. and Salinas, P. C. (1998). Inhibition of GSK-3β leading to the loss of phosphorylated MAP-1B is an early event in axonal remodelling induced by WNT-7a or lithium. *J. Cell Sci.* **111**, 1351-1361.

Martinez, A., Alonso, M., Castro, A., Perez, C. and Moreno, F. J. (2002). First non-ATP competitive glycogen synthase kinase 3β (GSK-3β) inhibitors: thiadiazolidinones (TDZD) as potential drugs for the treatment of Alzheimer's disease. *J. Med. Chem.* **45**, 1292-1299.

Noble, M., Lewis, S. A. and Cowan, J. (1989). The microtubule binding domain of the microtubule-associated protein MAP-1B contains a repeated sequence motif unrelated to that of MAP-2 and tau. *J. Cell Biol.* **109**, 3367-3376.

Noiges, R., Stroissnigg, H., Trancikova, A., Kalny, I., Eichinger, R. and Propst, F. (2006). Heterotypic complex formation between subunits of microtubule-associated proteins 1A and 1B is due to interaction of conserved domains. *Biochim. Biophys. Acta* **1763**, 1011-1016.

Okui, M., Ide, T., Morita, K., Funakoshi, E., Ito, F., Ogita, K., Yoneda, Y., Kudoh, J. and Shimizu, N. (1999). High-level expression of the Mnb/Dyrk1A gene in brain and heart during rat early development. *Genomics* **62**, 165-171.

Owen, R. and Gordon-Weeks, P. R. (2003). Inhibition of glycogen synthase kinase 3β in sensory neurons in culture alters filopodia dynamics and microtubule distribution in growth cones. *Mol. Cell Neurosci.* **23**, 626-637.

Paglini, G., Pigino, G., Kunda, P., Morfini, G., Maccioni, R., Quiroga, S., Ferreira, A. and Caceres, A. (1998). Evidence for the participation of the neuron-specific CDK5 activator P35 during laminin-enhanced axonal growth. *J. Neurosci.* **18**, 9858-9869.

Pigino, G., Paglini, G., Ulloa, L., Avila, J. and Caceres, A. (1997). Analysis of the expression, distribution and function of cyclin dependent kinase 5 (cdk5) in developing cerebellar macroneurons. *J. Cell Sci.* **110**, 257-270.

Qiang, L., Yu, W., Andreadis, A., Luo, M. and Baas, P. W. (2006). Tau protects microtubules in the axon from severing by katanin. *J. Neurosci.* **26**, 3120-3129.

Riederer, B. M. (2007). Microtubule-associated protein 1B, a growth-associated and phosphorylated scaffold protein. *Brain Res. Bull.* **71**, 541-558.

Ryoo, S. R., Jeong, H. K., Radnaabazar, C., Yoo, J. J., Cho, H. J., Lee, H. W., Kim, I. S., Cheon, Y. H., Ahn, Y. S., Chung, S. H. et al. (2007). DYRK1A-mediated Hyperphosphorylation of Tau: a functional link between Down syndrome and Alzheimer disease. *J. Biol. Chem.* **282**, 34850-34857.

Sato-Yoshitake, R., Shiomura, Y., Miyasaka, H. and Hirokawa, N. (1989). Microtubule-associated protein 1B: molecular structure, localization, and phosphorylation-dependent expression in developing neurons. *Neuron* **3**, 229-238.

Schliwa, M. and van Blerkom, J. (1981). Structural interaction of cytoskeletal components. *J. Cell Biol.* **90**, 222-235.

Stambolic, V., Ruel, L. and Woodgett, J. R. (1996). Lithium inhibits glycogen synthase kinase-3 activity and mimics wingless signalling in intact cells. *Curr. Biol.* **6**, 1664-1668.

Tejedor, F., Zhu, X. R., Kaltenbach, E., Ackermann, A., Baumann, A., Canal, I., Heisenberg, M., Fischbach, K. F. and Pongs, O. (1995). minibrain: a new protein kinase family involved in postembryonic neurogenesis in Drosophila. *Neuron* **14**, 287-301.

Tögel, M., Wiche, G. and Propst, F. (1998). Novel features of the light chain of microtubule-associated protein MAP1B: microtubule stabilization, self interaction, actin filament binding, and regulation by the heavy chain. *J. Cell Biol.* **143**, 695-707.

Trinidad, J. C., Thalhammer, A., Specht, C. G., Schoepfer, R. and Burlingame, A. L. (2005). Phosphorylation state of postsynaptic density proteins. *J. Neurochem.* **92**, 1306-1316.

Trinidad, J. C., Specht, C. G., Thalhammer, A., Schoepfer, R. and Burlingame, A. L. (2006). Comprehensive identification of phosphorylation sites in postsynaptic density preparations. *Mol. Cell Proteomics* **5**, 914-922.

Trivedi, N., Marsh, P., Goold, R. G., Wood-Kaczmar, A. and Gordon-Weeks, P. R. (2005). Glycogen synthase kinase-3β phosphorylation of MAP1B at Ser1260 and Thr1265 is spatially restricted to growing axons. *J. Cell Sci.* **118**, 993-1005.

Ulloa, L., Diaz-Nido, J. and Avila, J. (1993). Depletion of casein kinase II by antisense oligonucleotide prevents neuritogenesis in neuroblastoma cells. *EMBO J.* **12**, 1633-1640.

Woods, Y. L., Cohen, P., Becker, W., Jakes, R., Goedert, M., Wang, X. and Proud, C. G. (2001). The kinase DYRK phosphorylates protein-synthesis initiation factor eIF2Bepsilon at Ser539 and the microtubule-associated protein tau at Thr212: potential role for DYRK as a glycogen synthase kinase 3-priming kinase. *Biochem. J.* **355**, 609-615.

Yang, E. J., Ahn, Y. S. and Chung, K. C. (2001). Protein kinase Dyrk1 activates cAMP response element-binding protein during neuronal differentiation in hippocampal progenitor cells. *J. Biol. Chem.* **276**, 39819-39824.

Journal of Cell Science